3D Extended Logging for Geothermal Resources: Field Trials with the Geo-Bilt System

R. Mallan, M. Wilt, B. Kirkendall, P. Kasameyer

U.S. Department of Energy **May 29, 2002**

Lawrence
Livermore
National
Laboratory

3D EXTENDED LOGGING FOR GEOTHERMAL RESOURCES:
FIELD TRIALS WITH THE GEO-BILT SYSTEM

Robert Mallan and Michael Wilt
ElectroMagnetic Instruments, Inc. (EMI)
1301 46th Street, UCRFS
Richmond, CA, 94805, USA
rmallan@slb.com
mwilt@slb.com

Barry Kirkendall and Paul Kasameyer
Lawrence Livermore National Laboratory (LLNL)
Livermore, CA, 94550, USA
kirkendall1@llnl.gov
kasameyer1@llnl.gov

ABSTRACT

Geo-BILT (Geothermal Borehole Induction Logging Tool) is an extended induction logging tool designed for 3D resistivity imaging around a single borehole. The tool was developed for deployment in high temperature geothermal wells under a joint program funded by the California Energy Commission, Electromagnetic Instruments (EMI) and the U.S. Department of Energy. EMI was responsible for tool design and manufacture, and numerical modeling efforts were being addressed at Lawrence Livermore Laboratory (LLNL) and other contractors. The field deployment was done by EMI and LLNL.

The tool operates at frequencies from 2 to 42 kHz, and its design features a series of three-component magnetic sensors offset at 2 and 5 meters from a three-component magnetic source. The combined package makes it possible to do 3D resistivity imaging, deep into the formation, from a single well. The manufacture and testing of the tool was completed in spring of 2001, and the initial deployment of Geo-BILT occurred in May 2001 at the Lost Hills oil field in southern California at leases operated by Chevron USA. This site was chosen for the initial field test because of the favorable geological conditions and the availability of a number of wells suitable for tool deployment. The second deployment occurred in April 2002 at the Dixie Valley geothermal field, operated by Caithness Power LLC, in central Nevada. This constituted the first test in a high temperature environment.

The Chevron site features a fiberglass-cased observation well in the vicinity of a water injector. The injected water, which is used for pressure maintenance and for secondary sweep of the heavy oil formation, has a much lower resistivity than the oil bearing formation. This, in addition to the non-uniform flow of this water, creates a 3D resistivity structure, which is analogous to conditions produced from flowing fractures adjacent to geothermal boreholes. Therefore, it is an excellent site for testing the 3D capability of the tool in a low risk environment. The Dixie

Valley site offered an environment where the tool could locate near-well fractures associated with steam development.

The Lost Hills field measurements yielded a data set suitable for 3D imaging. The Geo-BILT data corresponded to existing conventional logging data and showed clear indications, in several depth intervals, of near-well 3D structure. Subsequent 3D inversion of these data produced a model consistent with non-planar water flow in specific layers. The Dixie Valley measurements identified structures associated with dike intrusions and water inflow at particular depths. Preliminary analysis suggests these structures are steeply dipping, which is consistent with the geology.

INTRODUCTION

Geothermal resource evaluation in boreholes has always been difficult due to the complex geology and hostile, downhole conditions. Using standard oil field logging devices has proven unsatisfying, as these are ineffective in non-layered geology and high temperature boreholes. In the past several years, a series of experimental induction resistivity tools were developed by EMI, in cooperation with researchers in Japan, for fracture detection and formation evaluation in geothermal wells (Sato et. al., 1996; Miura et. al., 1996). In this paper we describe the latest in this series of tools, the Geo-BILT.

The Geo-BILT project entails the development of a full tensor, extended induction logging device capable of operating in high temperature boreholes. The project was begun in 1999 with the tool design and numerical modeling. Tool manufacture proceeded in 2000 and was completed in February 2001.

In this paper, we describe the tool design and operation. We proceed to give results from two field tests and show interpretations that are consistent with the local geologies.

TOOL CHARACTERISTICS

Figure 1 is a schematic drawing of the Geo-BILT device. GeoBILT is designed so that the signal generation and data processing is mainly accomplished downhole. The surface station provides power, gives digital commands and receives a digital data stream from the tool.

The borehole tool consists of three separate sections: two electronic compartments and one antenna sonde. The electronic sections are housed in vacuum insulated dewars. These dewars are basically thermos bottles that isolate the interior from the exterior. In a high temperature environment, the interior temperature increases at roughly 6° C / per hour. This provides an operating range of 12-14 hours before cooling is required.

The housings for the antennas are made of a special high temperature fiberglass composite material that is stable up to 260° C. High temperature solder is also used for all electrical connections. The O-rings and greases used are stable at high temperature and minimize heat transfer.
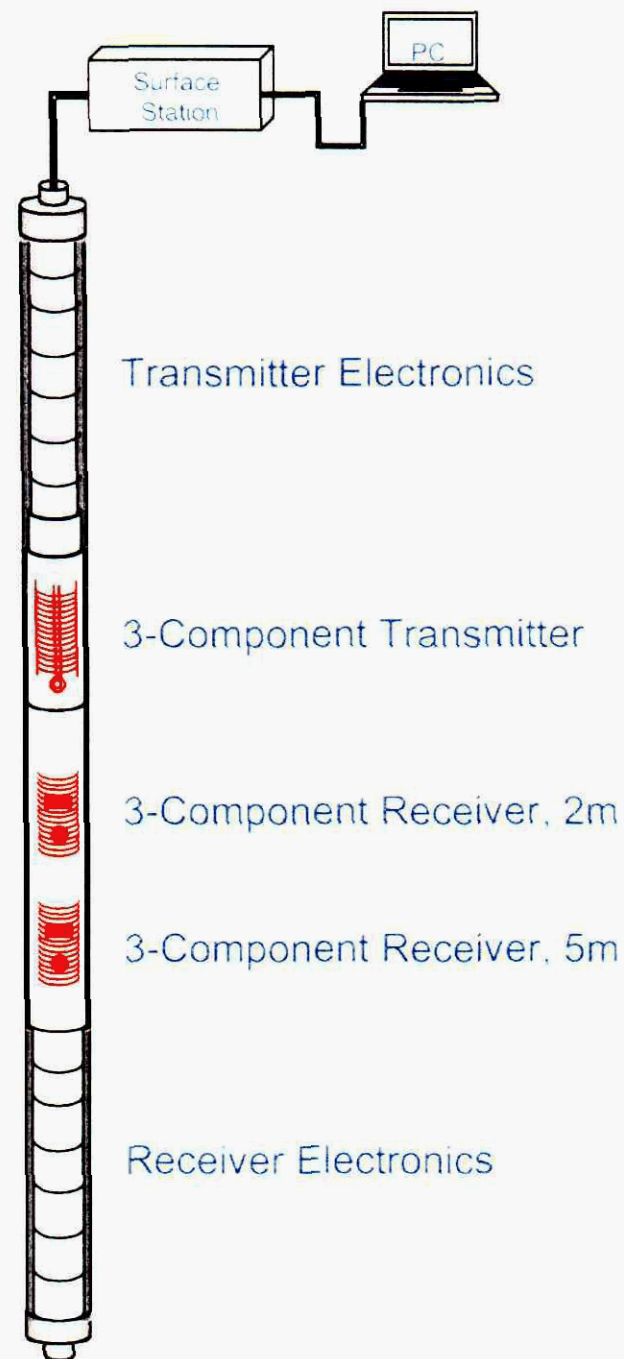
Figure 1: Schematic drawing of Geo-BILT tool.

The source antennas are coincident, multiturn coils wound around a common center with matched inductances, allowing them to be tuned with a single set of capacitors. The antennas are air-core coils wound around a machined frame made of high temperature fiberglass. They are roughly 1m long and the magnetic moment of all of the sources is approximately 10 A-m^2. This is sufficient source strength for operation at source-receiver offsets of up to 50 m.

The transmitter signal is generated downhole using a driver circuit controlled by the clock. The driver is basically a very efficient power supply switch that generates a square wave signal with a minimum of heat dissipation. The tool operates at 4 four frequencies: 2, 6, 16 and 42 kHz. At each frequency, the downhole computer selects a capacitor to connect in series with the coil. This capacitor tunes the coil, thereby dramatically reducing the impedance at the tuning frequency, and thereby increasing the current. Capacitive tuning of the square wave signal also results in the sinusoidal transmitter waveform.

GeoBILT has two three-component magnetic induction sensors separated at 2 and 5 m from the source. These sensors are multiturn coils each wound around a common center. The axial receivers are simple multiturn coils wound around a base; the transaxial receivers are made of small coils 3 inches by 1.5 inches with a mu-metal core. The sensors and attached amplifiers are designed for optimum sensitivity in the frequency range of 2-50 kHz.

GeoBILT also features a three-component magnetometer and accelerometer package for tool orientation. Three separate toroidal sensors are used as transmitter current monitors, and a series of temperature and voltage sensors are used for assessing the operating conditions. The magnetometers are necessary for triaxial operation because the tool spins freely during logging. Before the data can be interpreted, it is required that the sensors be rotated to known positions. This is done mathematically through the magnetic sensors.

The signals are channeled from all receivers and sensors into a downhole analog to digital converter (A/D) and computer module. Data are first digitized by a 16-bit, 4-channel A/D and averaged on the downhole computer. The Fourier coefficients are then transmitted to the surface along with a selected stacked digital time series and the tool status data. These data are collected on a laptop computer connected to the surface station.

The surface station supplies power to the transmitter and receives digital signals from the downhole computer. Power for the receiver section is supplied by a downhole battery pack. The battery pack was added after initial system tests demonstrated that a higher isolation is needed between the source and receiver sections to eliminate stray coupling. This isolation was accomplished by reducing as many wire connections as possible between the source and receiver sections. The only remaining connection between the source and receiver sections is a transformer-isolated clock line and one shielded twisted pair for communication.

TOOL OPERATION AND DEPLOYMENT

The Geo-BILT borehole tool consists of three major sections that range from 12 to more than 23 feet long (Figure 1). Tool assembly is accomplished by laying the pieces horizontally on tool stands and fitting together the joints using hand tools; the process takes about an hour on site. When fully assembled the tool is more than 45 ft long and must be hoisted as one piece. We have devised a special rolling sling for accomplishing this (Figure 2).

The tool is deployed using standard 7-conductor wireline cable and an encoder/counter for depth control. Due to its length, a 60 ft crane is required to deploy the tool. After assembly and initial testing, the tool is typically hoisted and positioned over the well. We then collect "free space" data at the frequencies selected for logging, and these data are used as part of the calibration corrections.

The borehole is logged while the tool is moving. The logging speed ranges from 10 to 20 ft per minute depending on the frequency and stacking. At a rate of 10 ft/minute, we can obtain a full tensor measurement about every foot.

Figure 2: Field deployment of Geo-BILT tool.

GEO-BILT FIELD TRIAL AT LOST HILLS, CALIFORNIA

The initial deployment of Geo-BILT occurred from May 8-11, 2001 at the Lost Hills oil field in southern California at leases operated by Chevron USA (Figure 3). The Lost Hills oil field is located at the western margin of the San Joaquin basin in Kern County, California (Stosur and David, 1976). Production is mainly from an upper member of the Miocene Monterey Formation known as the Belridge Diatomite. This reservoir is comprised of diatomaceous mudstone (diatomite) that averages 800 ft in thickness and is characterized by very low matrix permeability, high porosity (35-65%) and good oil saturation (50%).
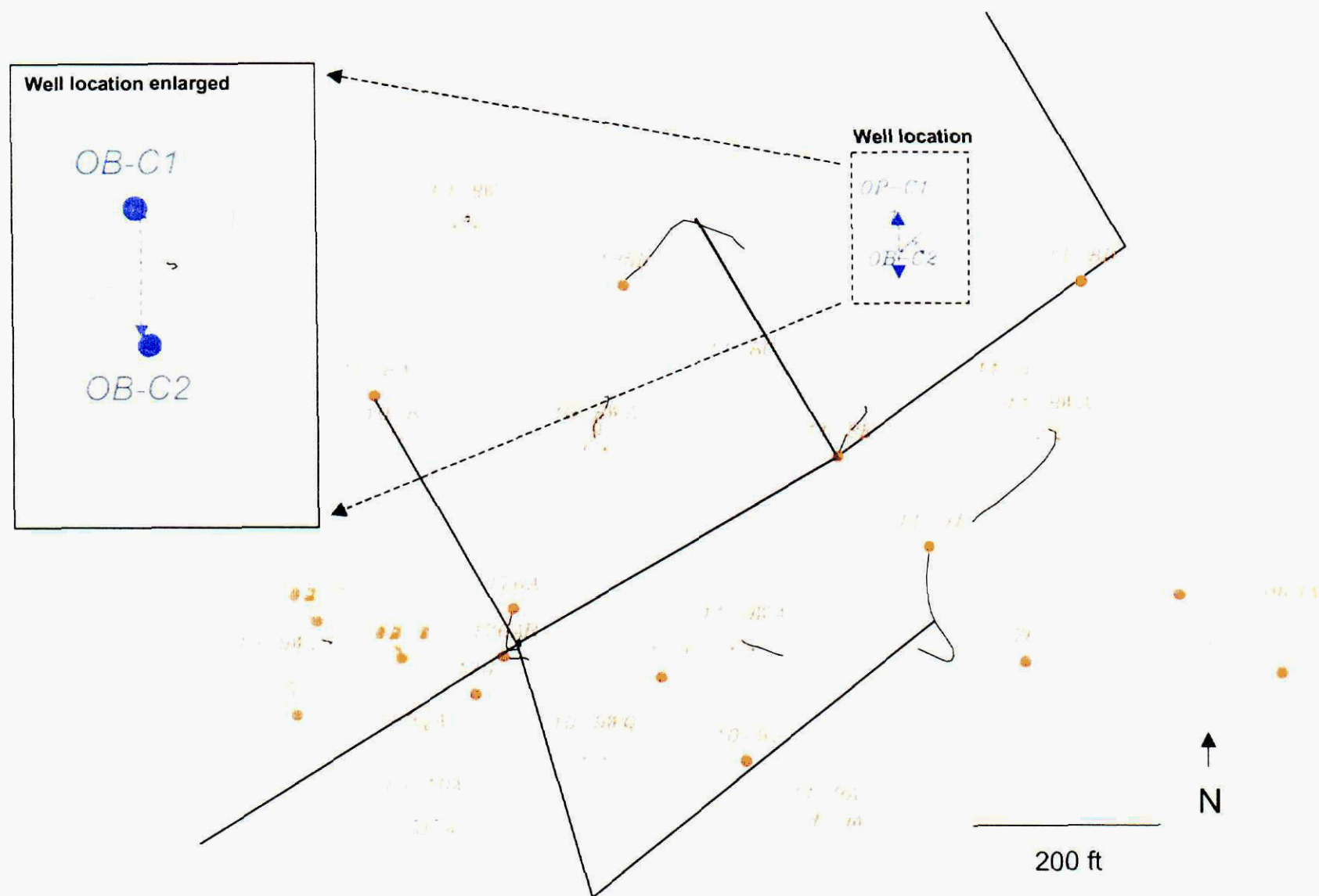
Figure 3: Base map: Chevron-Lost Hills.

Data were collected in a fiberglass cased observation well adjacent to an active water injector. The flood alters the formation resistivity, due to the lower resistivity of the injectate, thereby creating a 2D and 3D resistivity structure that may be imaged from the observation well. We note that the injection well (11-8w) is hydraulically fractured resulting in a vertical fracture trending roughly North 60 E (Figure 3).

The injected water is a combination of produced water and make-up water from a shallower and less saline source. The overall fluid is 30 percent more resistive than the formation water, but the injected fluid will still dramatically reduce the formation resistivity as it fills up void space or mobilizes oil or gas. In Figure 4 we show deep induction logs from wells 11-8wr and 11-8w, measured before and after the start of the water injection, respectively. The difference between these two logs is due to the effect of the water injection on the near well formation. The logs indicate resistivity decreases of up to 50 percent in several layers where the water injection is significant. In particular, the F, H and K intervals show the greatest change due to the flooding.

Mallan, Wilt, Kirkendall and Kasameyer

Deep Induction Resistivity

Marker units

F

G   11-8w

H

J   11-8wr

K
I
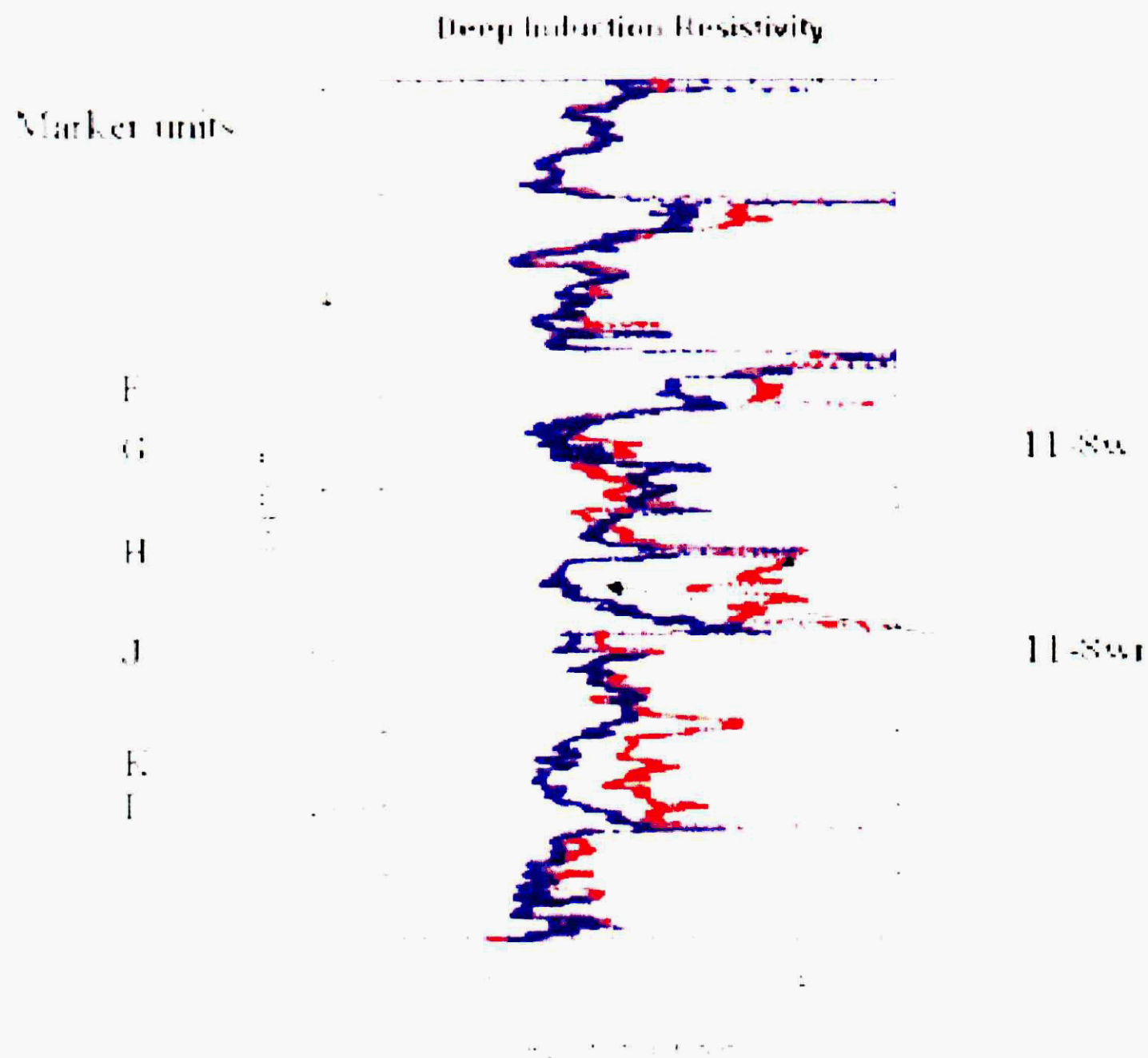
Figure 4: Induction resistivity logs: comparison between 11-8w and 11-8wr.

Field experiment

The Geo-BILT system was used to log two intervals, the complete reservoir (1200-2100 ft) and the main water flooded interval (1400-1800 ft). Data were collected at all four frequencies, and all logs were measured at least twice. These repeated logs help to establish repeatability and to identify conditions such as thermal drift and capacitive coupling. The complete set of logs required about 16 hours over two days. The tool worked reliably for the entire survey.

Data processing was completed in two stages: 1) calibration adjustment and 2) tool rotation. In the calibration adjustment, we adjust the data with respect to measurements made in free space. The final processing consists of tool rotation, using the thee-component magnetometer data to orient the tool axes to geographic north (X coordinate).

Results

Figure 5 shows apparent resistivity logs, with repeats, from the vertical source and the 2m and 5m offset vertical sensors. We also show the logs from the commercial (Halliburton) deep

induction resistivity log, measured several months prior in the same well. The plots show a good correlation with the commercial log, although both Geo-BILT logs are somewhat smoother due to the longer receiver offsets. The slight variation between the repeated logs is most likely due to thermal drift. We have not completed a full system calibration so the thermal constants are as yet unknown. Figure 6 shows the apparent resistivity logs for the horizontal component, maximum coupled sources and receivers (Hxx and Hyy) in the same well, with repeats.

The Hxx and Hyy logs are quite different in appearance to the vertical logs in Figure 5 and somewhat different from each other. The horizontal logs appear sharper and choppier than the vertical logs, and although many layers correlate, others do not. Note that the 2m and 5m offset logs appear quite different from each other. The 2m plots are sharper and show smaller swings at layer boundaries. We suspect that these logs are responding to the thinner layers.

The variance of the repeated horizontal logs is considerably higher than the vertical logs. This is probably due to the fact that each log is in fact the rotated resultant of two individual logs. We therefore see the combined affect of the drift on both logs as well as the result of the propagation of any calibration differences between the sensors and sources.

The logs Hxx and Hyy are similar to each other in overall appearance over much of the section but quite different in several specific zones. For example, at depths between 1600 and 1750 ft, the logs are quite different in appearance. We note that these depths correspond to the largest water influx from the adjacent water injector, and the differences between the logs might correspond to an injection induced anisotropy (i.e. 3D structure due to water flooding).

Samples of the null coupled logs (Hzx and Hzy) are provided in Figure 7. Here we show the amplitude of the horizontal fields from the vertical source for the entire reservoir depth (1200-2100 ft). These fields are theoretically zero for a horizontally layered structure about a vertical well, but they are clearly not zero here. In particular, there are significant anomalies centered at depths 1350, 1450, 1700 and 1925 ft. We note that these depths correspond to layers most affected by water flooding from the adjacent injector (Figure 4). Also note that the characteristics of the null fields are different in each of these anomalous zones as evidenced by the variation of the X and Y component logs. This suggests that the flow direction and characteristics are different in each interval. Although the magnitude of these null coupled fields is quite small, between 0.1 and 2 percent of the direct coupled field, the repeated logs show that these data are very reproducible. In fact, from these data we estimate that the reproducibility is roughly 100 parts per million.
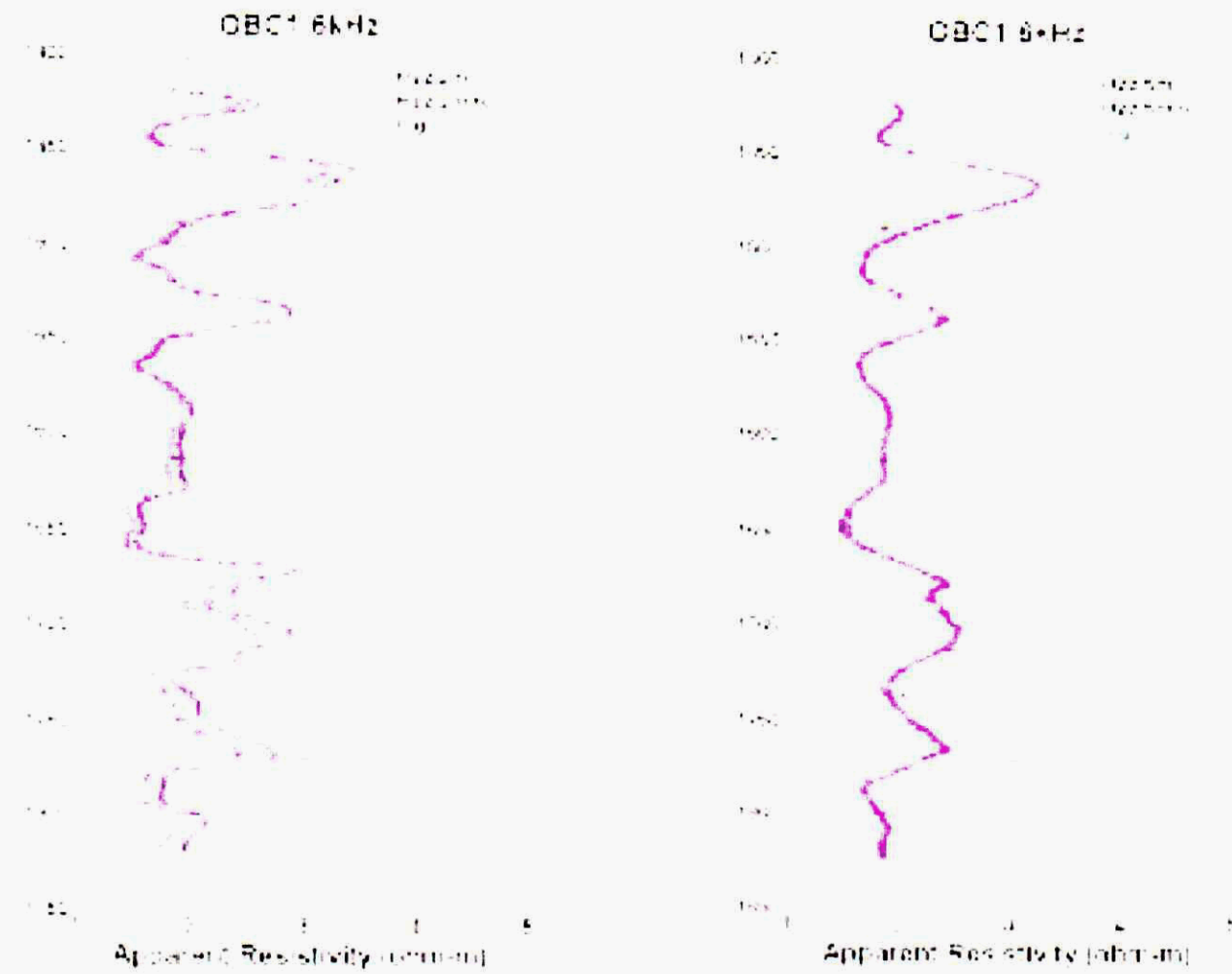
Figure 5: Geo-BILT logs of Tz-Rz for 2 m and 5 m separations.
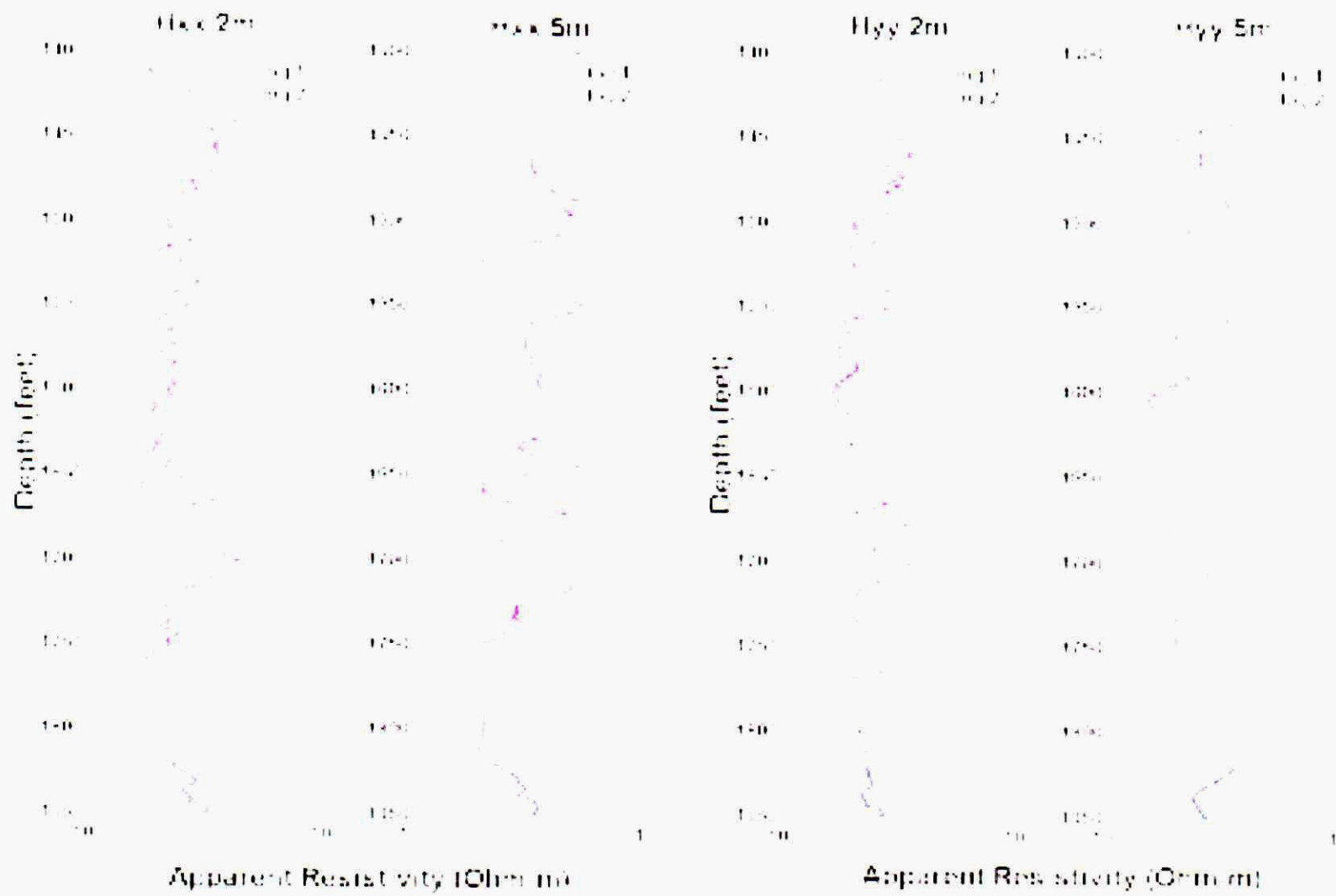
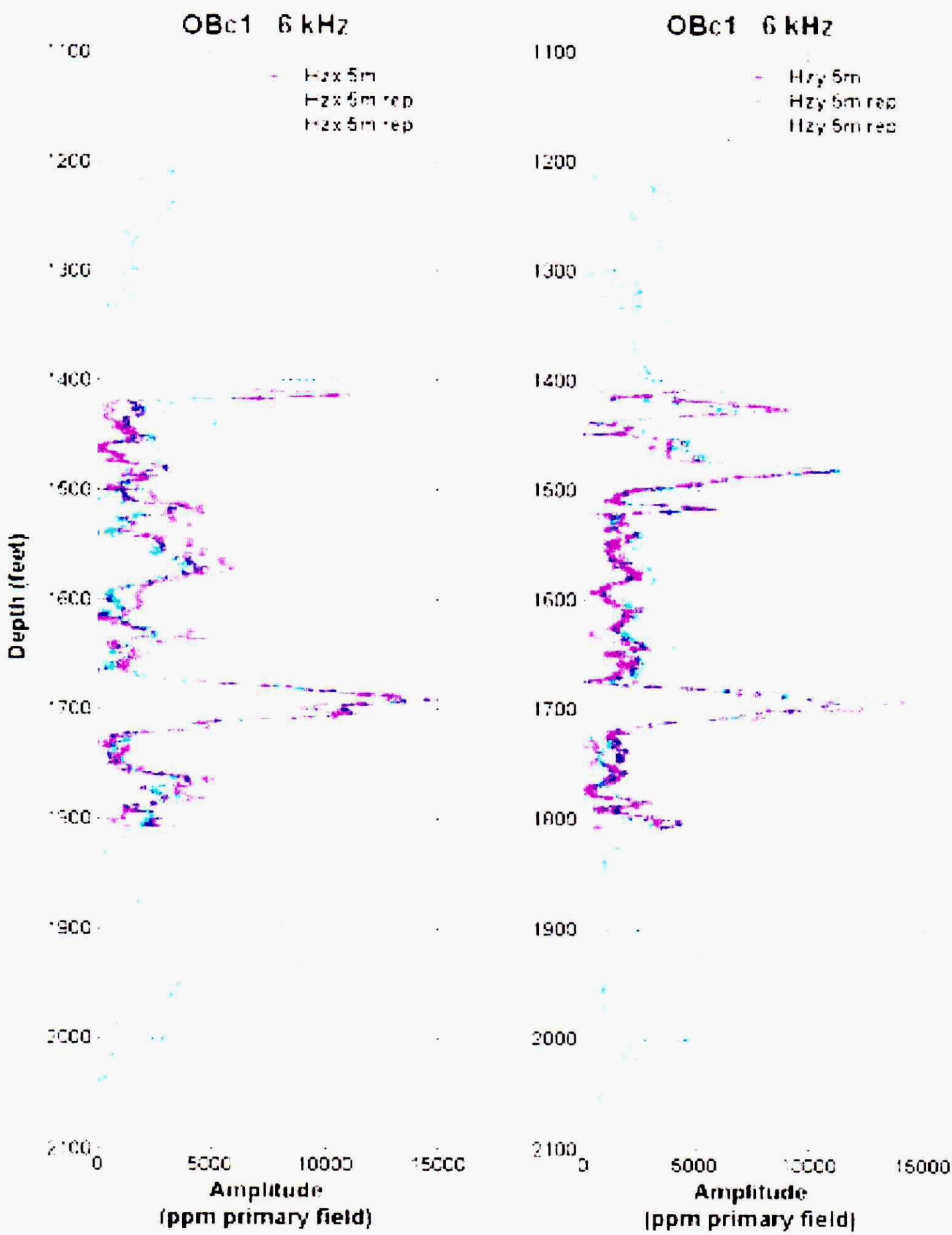**Figure 6: 6 kHz Geo-BILT logs from OBC1 of Tx-Rx and Ty-Ry for 2 m and 5 m separations.**

Figure 7: Geo-BILT logs of Tx-Rx and Tz-Ry for 2 m and 5 m separations.

Data Interpretation

Geo-BILT results are interpreted in two ways. First, the apparent resistivity logs are examined qualitatively by matching them to the geologic sections. This allows for some average determination of saturations. The cross-coupled logs are then examined for near well anomalous zones that may be related to fractures or in this case water flooded horizons. A more rigorous interpretation is the application of these data in a 3D inversion. Here we wish to reconstruct a 3D resistivity distribution around the borehole that honors both the data as well as being consistent with the known geology. Geo-BILT data were fit with a 3D inverse code, INV3D, developed by Sandia Laboratories (Alumbaugh and Newmann, 1996). Although this code has been used in crosshole (Wilt at al, 2000) and surface data, these are the first single well data used for 3D inversion.

Given the computational intensity of 3D inversion, we applied the 3D inversion to the data in the depth interval from 1400-1800 ft, where the largest 3D effects were observed in the data and where there is strong evidence of water flooding at the injection well (Figure 4). For simplicity we used only the vertical component transmitter and all three orthogonal receivers at the 5 m offset. These data were fit in stages. We first applied a layered inverse code to fit the vertical component data (ZZ). Using this as a starting model we fit the null component data to a 3D resistivity distribution. The final solution was then checked against all data. This procedure, although somewhat laborious, was found to be more effective in the long run.

Even for this limited depth interval the 3D inversion was a lengthy process. Each inverse model required 2-5 days for convergence. In addition the results were dependent on the weighting of data, the starting model and the noise level and calibration correction of collected data. The results were that numerous runs were made over a two month period to produce the model shown in Figure 8.

In Figure 8 we show a South-to-North cross-sectional view of the 3D resistivity distribution near well OBC1 between 1400 and 1800 ft in depth. The final 3D model is consistent with the logs and the geology, and the data fit is adequate (within 10 percent).

The main feature of the model is low resistivity zone that extends southwards and eastward from the well from the well towards the injection fracture. The model also shows a higher resistivity body encircling the observation well and centered just north and west of it. The logs in Figure 4 show that the undisturbed formation is roughly 4-4.5 ohm-m, and the fully swept formation is approximately 1.8 ohm-m. The 3D model shows that well OBC1 is located in a transitional zone between these two extremes. The injected water is probably not moving as a coherent front; some of it has injected saltwater has moved past OBC1 and some has not reached the well.

We feel that the final model is a good portrayal of the resistivity structure near well OBC1, and from this we can ascertain at least two things. First is that the inversion defined an anomalous zone confined to depth range from 1660 to 1740 ft within 25 ft of the wellbore. The second is that the resistivity of this zone is greater north and east of the well.

We expect that the 3D single well inversion results will become more enhanced as more data (Hxx and Hyy) are incorporated into the inversion; this of course also relies on better computational resources in the future.
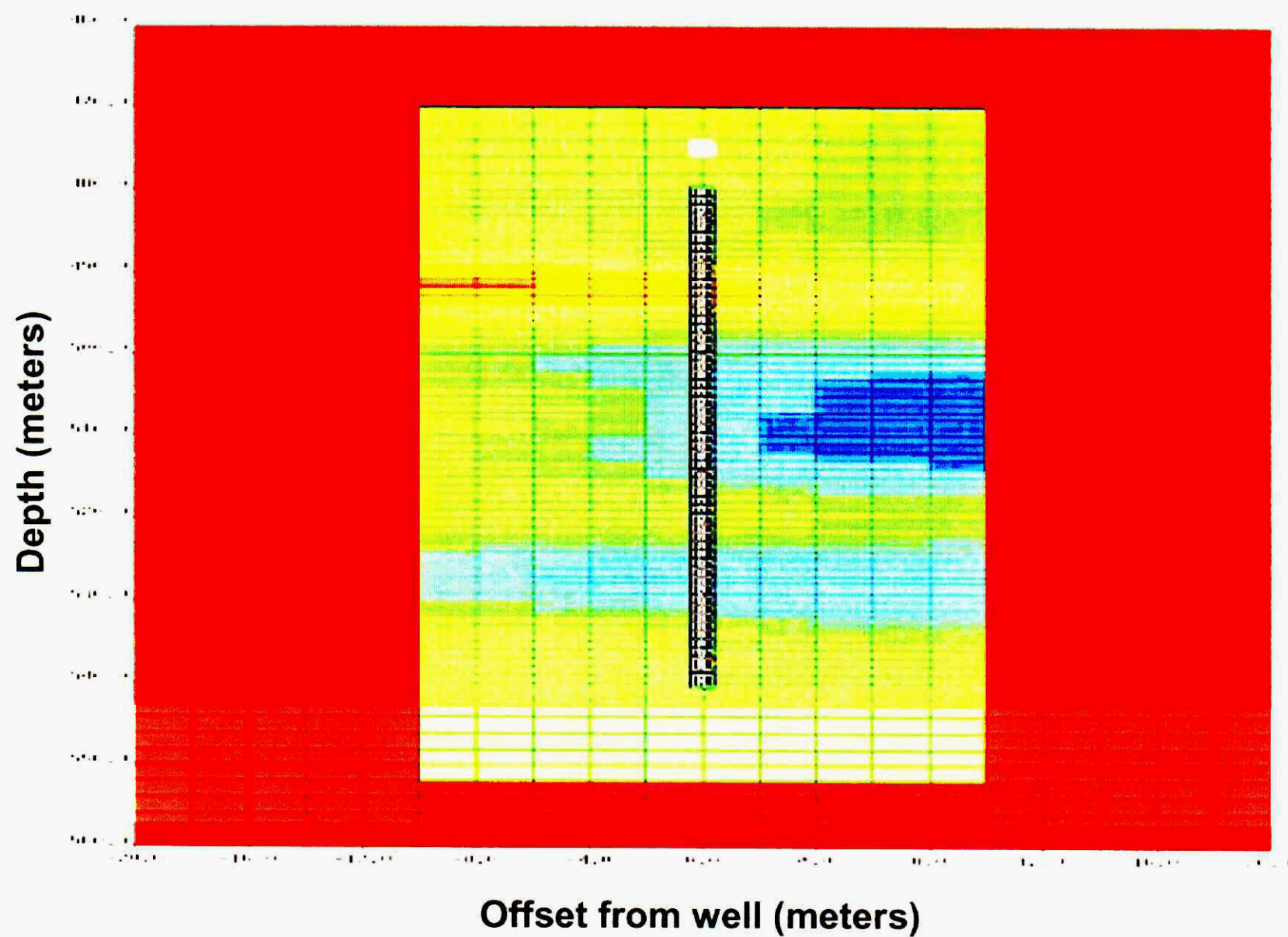
Figure 8: South-North section of 3D inversion for Geo-BILT data collected in well OBC1 using 6 kHz transmit frequency and 5 m transmitter-receiver separation.

DIXIE VALLEY FIELD EXPERIMENT

Our second field application was in geothermal wells in the Dixie Valley field of central Nevada (Figure 9). In this case, our objective was to operate GeoBILT in a high temperature environment and in an area where the tool could locate near well fractures associated with steam development.
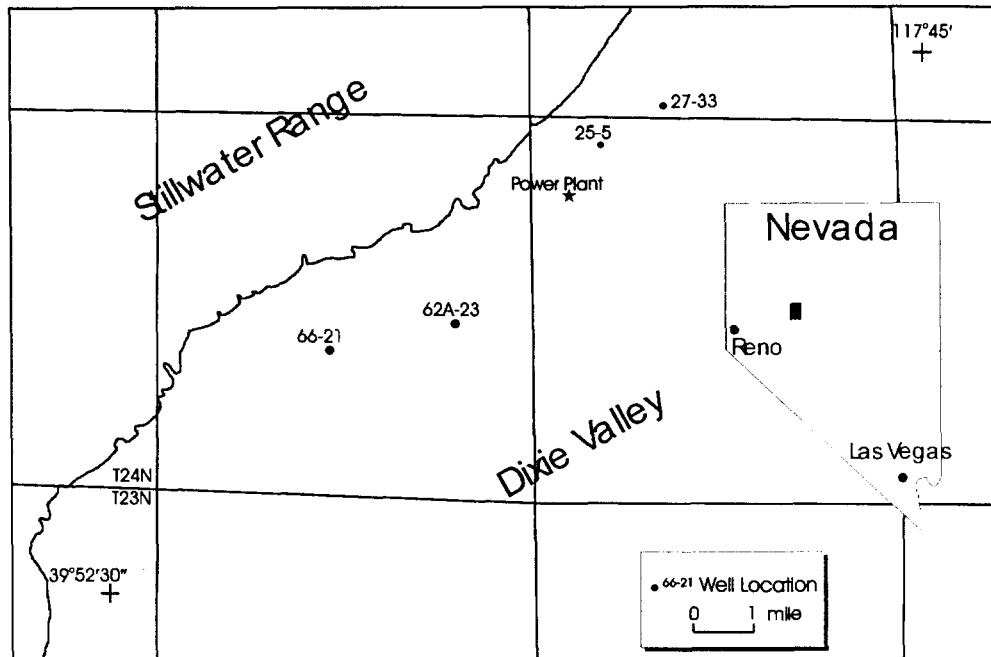
Figure 9: Base map for the Dixie Valley survey.

The Dixie Valley geothermal field was discovered in 1970 and has been in operation for more than 15 years. The field is presently operated by Caithness Power LLC and it produces approximately 65 megawatts from a power plant fed by more than 20 wells centered around the present power facility.

Effective steam wells are 8,000-10,000 ft deep and are completed in fractures associated with the range front fault in this basin and range valley. Wells are completed in volcanic and metasedimentary rocks and bottom hole temperatures are from 230-260° C. The flow rates are strongly dependent on the nature of the fractures encountered. If the fractures are open, the well can flow at rates exceeding 300,000 lbs/per hour. In some areas, however, the fractures are closed and the wells do not flow.

Wells 66-21 and 62A-23 are located 4-6 miles south of the existing producing field along the range front (Figure 9:). Both of these wells are hot but neither produces fluids. The bottom hole temperatures in well 66-21 are more than 220° C and more than 250° C in well 62A-23. South of the producing field, where these well are located, there is strong geological evidence for additional steam deposits and several surface manifestations. With one exception, however, the exploration wells in that part of the field are hot but dry.

13

Mallan, Wilt, Kirkendall and Kasameyer

The stratigraphic section in well 66-21 consists of 4,500-5,000 ft of alluvial sediments underlain by a sequence of volcanic, metamorphic and plutonic rocks. The structural relationships between the various basement rock units are quite complex as evidence by geological studies in the adjacent Stillwater range (ref). The open hole section of the well spans from 7,200-10,000 ft, but there is a constriction at a depth of 8200 ft, which makes it impossible to log below this depth. We are therefore restricted to logging to the 1000 ft interval between 7200 and 8200 ft. This interval may be important, however, as there are several zones within these depths where fluid is entering the well.

In Figure 10, we show the original induction resistivity log and a lithologic log in the interval that GeoBILT was logging. The lithologic sequence in this interval mainly consists metasediments and volcanic rocks with several sequences of granitic rocks, which may in fact be intrusive dikes. The induction log in this interval is fairly nondescript and averages between 50 and 100 ohm-m, with the exception of the interval near 7850 ft and another zone at 7600 ft. Both of these intervals correspond to a change in lithology, from metasediments to granitic rocks. We surmise that there is significant dike intrusion in this interval.
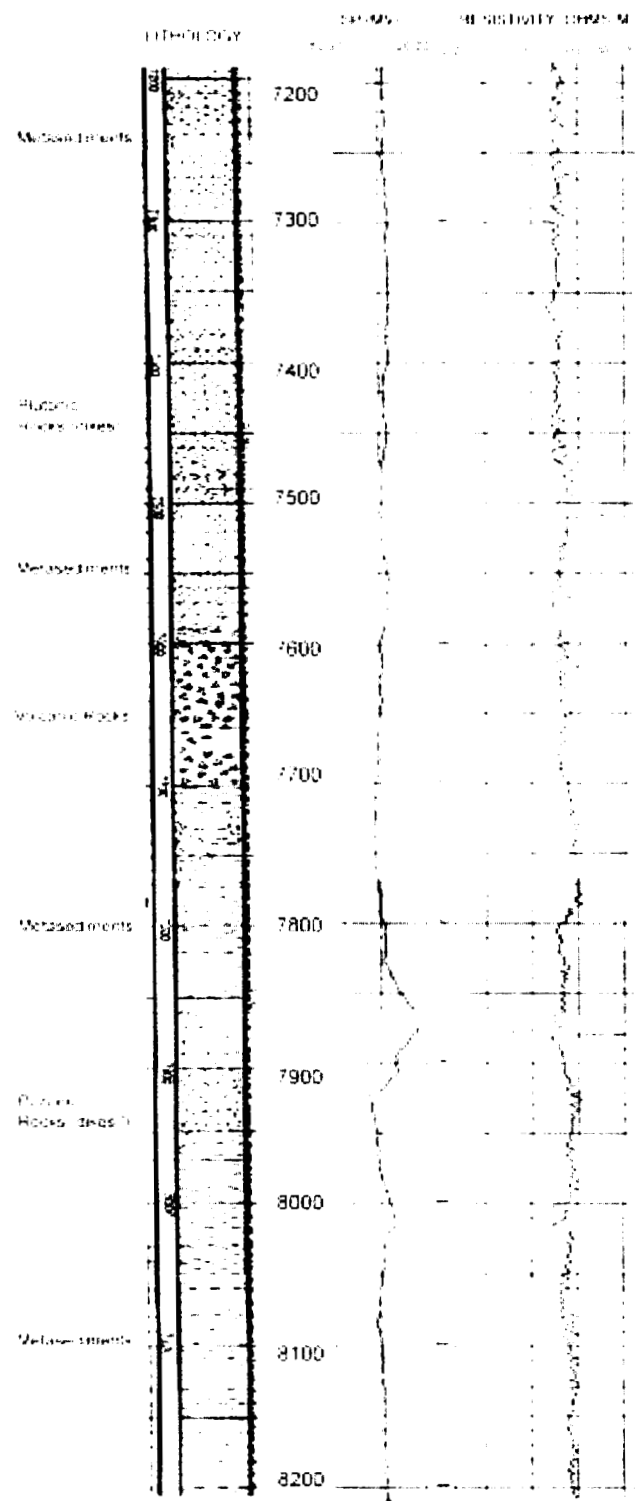
Figure 10: Resistivity and lithologic log for well 66-21.

Mallan, Wilt, Kirkendall and Kasameyer

Field Survey

GeoBILT was deployed in well 66-21 on April 10-12, 2002 (see Figure 9:). The plan called for the collection of three logs using all field components. Two of the logs would be duplicates so that we can measure the tool repeatability in the high temperature environment. The remaining log was collected at a different frequency.

The external temperature ranged from 200° C to 220° C with the highest temperatures at the bottom of the interval. The internal tool temperature, of the electronic circuits within the insulated dewar, ranged from 60° C at the start of logging to more than 120° C at the end. We found that the temperature within the electronics dewar increases at approximately 10° C/ hour, allowing us 6-7 hours of logging time per deployment. The tool experienced failures at temperatures above 120° C and some of the electronic components that were rated to 125° C failed at those temperatures. One problem is that the receiver section of GeoBILT is powered by batteries and the tool begins to operate (and heat up) as soon as the battery pack is connected. Because the tool must be positioned below a depth of 8,000 ft using a 120 ft/minute, GeoBILT is typically powered on for about 2 hours before logging begins, thereby reducing the logging time to about 5 hours.

The collection of the three logs required about three days, including frequent repairs of electronic components due to temperature induced failures. We believe that the highest quality logs were acquired early in the data collection.

After operations were complete in well 66-21 the tool was deployed in well 62A-23. This well is located about 4 miles south of the main field in the dry lakebed at the west side of the valley. This well is deeper and hotter than 66-21 with reported temperatures exceeding 250° C. We first deployed a dummy tool to determine the integrity of the well and found that it was open to more than 10,000 ft. We next deployed GeoBILT in 62A-23, but the tool failed early in the initial deployment and we were not able to repair it in the field. The survey was therefore terminated at that point.

Data Collection and Interpretation

We present the GeoBILT logging results as a series of apparent resistivity plots for the different field components. The GeoBILT axial logs are equivalent to the standard induction logs, whereas the transaxial and null coupled logs potentially offer new information on the near borehole structure.

In Figure 11, we show the 2 m and 5 m offset GeoBILT axial apparent resistivity logs collected at 6 kHz in well 66-21. We observe that the axial GeoBILT logs are quite similar to the original induction logs in Figure 10. In this depth interval, the axial logs are largely featureless except for the anomalous zone encountered at a depth of 7860 ft and a smaller one at 8200 ft. It is interesting to note that many of the lithologic units do not have an expression in the axial resistivity logs.

According to the lithology log, the anomalous zone at 7860 ft corresponds to a change from metasediments to a granite diorite. We believe that this boundary probably corresponds to a dike intrusion rather than a stratigraphic boundary.

16
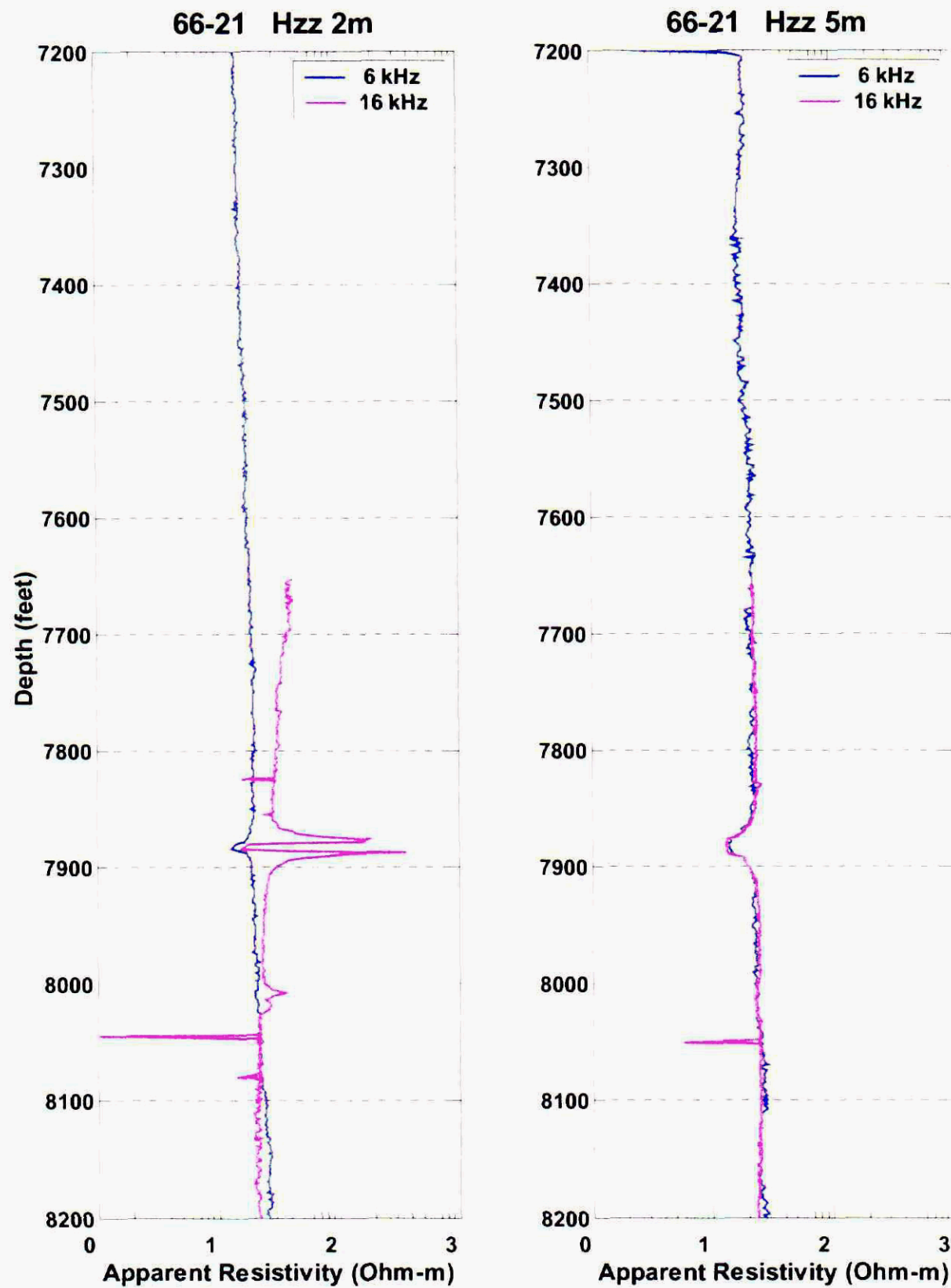
Figure 11: GeoBILT axial apparent resistivity logs for 2m and 5m offsets.

The transaxial logs show considerably more character and are more variation than the vertical logs (Figure 19). We see significant structures at depths of 7450, 7550, 7850 and 8220 ft. The log provides plots for both 6 kHz and 17 kHz measurements and it is clear that they seem to track the same structures.

The clear question is why do the transaxial logs appear to be sensitive to structure transparent to the axial logs. The most likely possibility is that the near well structures are dipping. For a horizontal layer, the axial sensors are optimally positioned to induce current into the layer; for a

dipping layer, this can be substantially reduced, and for a vertically dipping layer, the transaxial sensors are ideally oriented.

We tested this assertion with a simple layered Earth model. We computed axial and transaxial apparent resistivity logs for a flat lying, low resistivity layer in a uniform medium, and for the same model with a 60-degree dip. This layer might represent a thin hot fracture zone, for example. The model used a 5 m source-sensor spacing and a frequency of 6 kHz, the same as GeoBILT.

For the horizontal layer, we observed that the axial and transaxial fields produce roughly the same response from the layer. For the dipping layer, however, the transaxial configuration is more than two times as sensitive to the target. This means that for a steeply dipping section, the transaxial configuration is more sensitive and more definitive.

The logs and this simple model simulation suggest that the structure near well 66-21 is dipping, at about 60 degrees. The correspondence of the low resistivity zones in the GeoBILT logs with the granitic rock annotated in the lithology log suggests that these granitic zones are probably intrusive dikes. We can get a bit more information by examining the null-coupled logs.

In Figure 13, we show the null-coupled ZY logs (Y sensor directed eastwards) in this well. The logs represent the signal measured in an orthogonal sensor to the source. The logs are therefore zero in a uniform or layered space but they are very sensitive to nonuniform structure around the wells, such as fractures or steep dip. Typically these logs must exceed 0.5 percent of the direct coupled field to represent significant structure and it is important that the logs be repeated to determine level at which features reproduce. We are gratified that the 6 and 16 kHz null-coupled data agree at levels above 0.5 percent, especially in the ZY component.

The ZY (east receiver) and ZX logs (north receiver) are fundamentally different logs in this well. The ZX log is relatively small for the entire interval, whereas ZY is significant in several intervals. This indicates that the causative structure lies mainly west of the well and there is little component directly to the north.

Examining the lithology logs in Figure 10, we can see a good but rough correlation of the null coupled anomalies and the granitic lithology. This is further evidence that the granitic annotation refers to intrusive dikes and that these dikes are dipping bodies associated with fractured country rock.

We feel that GeoBILT data from these logs in 66-21 provided some new information unavailable from the standard induction logging. GeoBILT provided information on the nature of the anomalies as well as the dip and orientation of the causative structure.
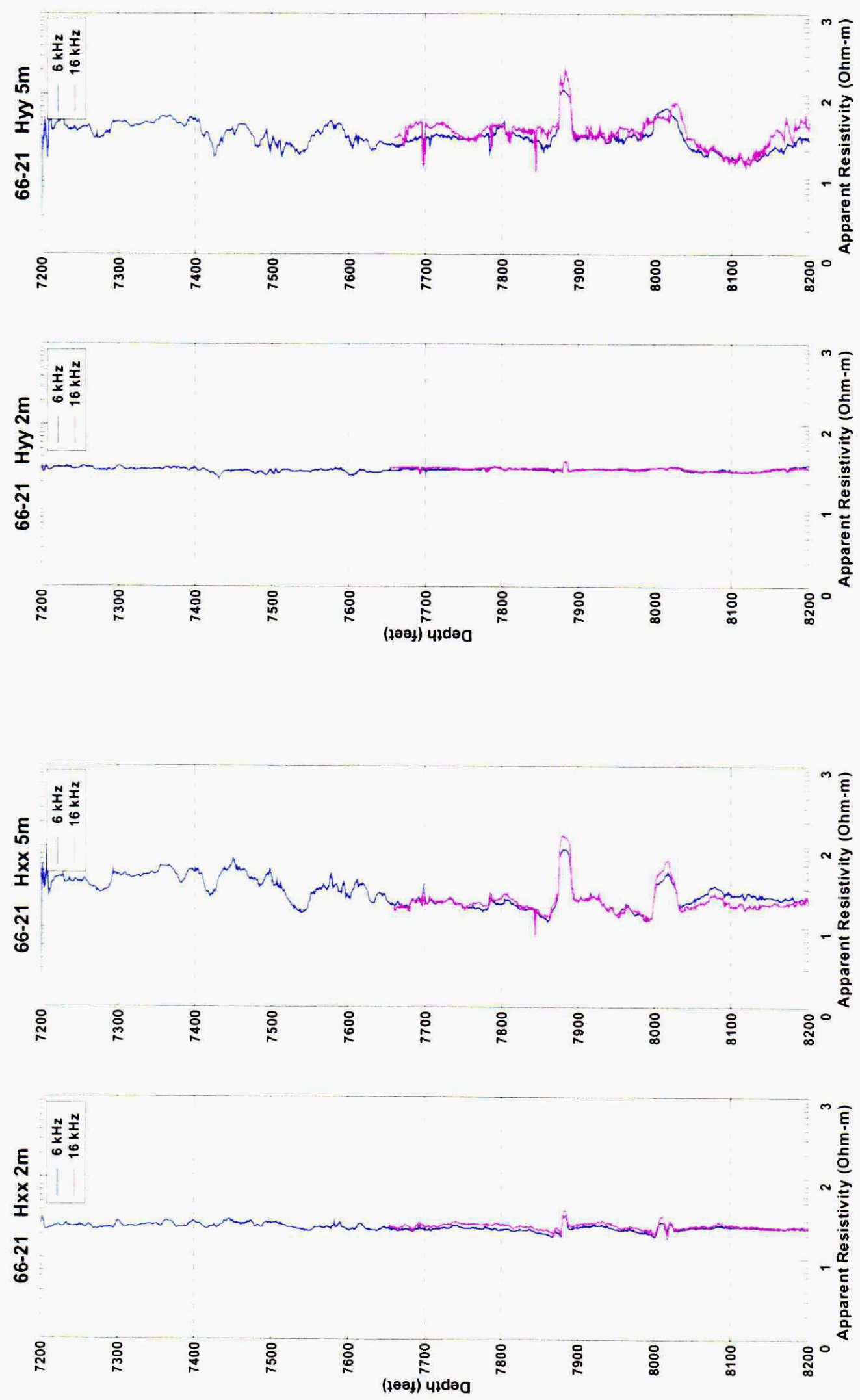
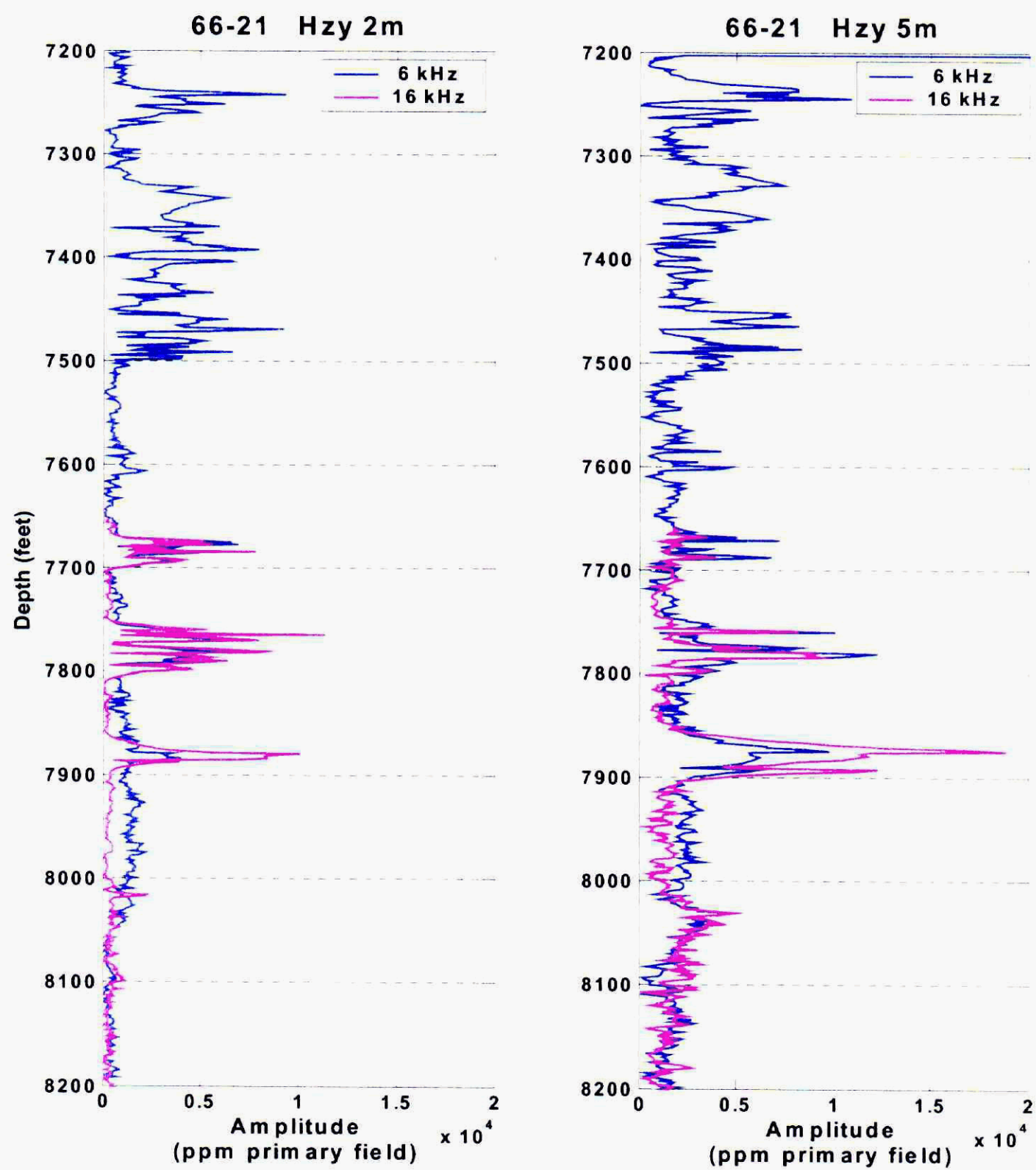Mallan, Wilt, Kirkendall and Kasameyer

Figure 12: Transaxial logs.

19

Figure 13: Null-coupled logs.

CONCLUSIONS

The development of GeoBILT was a long complex process that culminated with the manufacture of a working prototype logging device. This devise was used in two field trials, and in each we feel it provided information unavailable with any other logging technology.

In Lost Hills, we used GeoBILT data to construct a near well 3D resistivity model consistent with water flow from a nearby water injection well. The model is very useful in identifying horizons and flow paths to the water injection used for oil recovery and pressure maintenance. In the high temperature Dixie Valley geothermal field, GeoBILT data was able identify steeply dipping structure associated with dike intrusion and water inflow in particular depth horizons.

The potential benefits of this technology for both oil and gas and geothermal development are clear. The logs truly make the most of the access provided by the drill hole. GeoBILT can see 2 and 3D formation structure at substantial offsets from the well bore and clearly identify near well fractures.

ACKNOWLEDGEMENTS

REFERENCES

Alumbaugh, D.L. and Newman, G.A.,1996, 3D Massively Parallel Electromagnetic Inversion Part B: Analysis of a Cross Well EM Experiment, *Radio Science* (1996).

Alumbaugh D.L. and Wilt, M.J., 2000, A Numerical Sensitivity Study of Three Dimensional Imaging from a Single Borehole. Petrophysics 42 no1 pp19-31

Miura, Y., Osato, K., Takasugi, S., Muraoka, H., and Yasukawa, K., (1996), "Development of the Vertical Electro Magnetic Profiling (VEMP) Method," Journal of Applied Geophysics, **35**, 191-197.

Sato, T., Osato, K., Takasugi, S., and Uchida, T. (1996), "Development of the Multi-Frequency Array Induction Logging (MAIL) Tool," Geothermal Resources Council Transactions, **20**(9), 637-642.

Stosur, J.J. and David, A., 1976, "Petrophysical Evaluation of the Diatomite Formation of the Lost Hills Field, California," *Journal of Petroleum Technology* 1138.

Wilt, M., Zhang, P., Morea, M., Julander, D. and Mock, P., 2000, Using Crosswell Electromagnetics to Map Water Saturation and Formation Structure at Lost Hills. Society of Petroleum Engineers (SPE) paper 68802.

Zhdanov, M. and Fang, S., 1997, computer code QL3DEM.